JOURNAL OF CATALYSIS 139, 468–481 (1993)

Acidity of H-Y Zeolites: Role of Extralattice Aluminum

PRASAD V. SHERTUKDE,* W. KEITH HALL,† JEAN-MARIE DEREPPE,*,[1] AND GEORGE MARCELIN*,[2]

*Department of Chemical and Petroleum Engineering, and †Department of Chemistry, University of Pittsburgh, Pittsburgh, Pennsylvania 15261

Received August 19, 1991; revised September 18, 1992

The nature of extralattice aluminum and its effect on acidity in zeolites was studied. A series of zeolites (some commercial), dealuminated by various methods, were obtained having Si/Al ratios between 1.5 and 20. These were characterized using volumetric sorption, XRD, AA, NMR, and reaction studies. Samples dealuminated using ammonium hexafluorosilicate were found to contain little or no extralattice aluminum. In contrast, steam-dealuminated zeolites had large amounts of extralattice aluminum. In some cases a significant portion of the extralattice aluminum was unobservable by ^{27}Al NMR, suggesting the existence of an aluminum species of low symmetry. Proton NMR indicated that all the protons were associated with the lattice aluminum atoms. Depending on the preparation history, different groups of H-Y zeolites exhibited different maxima in catalytic activity as a function of aluminum content. The maxima in catalytic activity for *n*-pentane cracking was found to be a function of both lattice and extralattice aluminum contents.

INTRODUCTION

The total acidity of zeolite catalysts may be considered to be a contribution of both an extensive factor representative of the number of acid sites and an intensive factor representative of the strength of the individual sites (*1, 2*). For structurally pure hydrogen-zeolites, the nature of acid sites is conceptually well defined. In that case Brønsted acidity is associated with the labile protons in the neighborhood of tetrahedrally coordinated lattice aluminum sites (*3*). Thus, the extensive factor of acidity is simply the number of protons held by the lattice aluminum per unit volume. Already in 1965 it was recognized (*3*) that the intensive factor could be greatly enhanced by the simple process of partial dehydroxylation which reduces the extensive factor.

In high-silica zeolites the lattice aluminum atoms are far apart from each other, and thus it may be expected that all acid protons would have about the same environment and thus have equal acid strength. This idea has been supported by studies involving adsorption of bases such as alcohols and amines on H-ZSM-5, H-ZSM-12, and H-mordenites (*2*), as well as hexane cracking and cumene dealkylation studies (*4, 5*). In the reaction studies a linear increase in activity with lattice aluminum concentration was observed, suggesting that each lattice aluminum corresponded to one acid site and all acid sites have the same intensive factor (acid strength).

There are many factors which may affect the intensive factor of the acidity in zeolites. For example, it has been well documented (*4–11*) that an optimum aluminum concentration exists in zeolites which corresponds to maximum acidity. Although further increasing the lattice aluminum concentration results in an increase in the extensive factor, the intensive factor is reduced due to delocalization of the negative charge density on the lattice.

[1] Permanent address: Laboratorie de Chimie Physique et Cristallographie, Université de Louvain, Louvain-la-Neuve, Belgium.

[2] To whom correspondence should be addressed.

0021-9517/93 $5.00

It has also been established that the presence of extralattice aluminum formed during dealumination can affect the intensive factor of zeolites (*5–8*). This was clearly demonstrated by Lago *et al.* (*5*) on ZSM-5 catalysts, in which dealumination using mild steaming resulted in a fourfold increase in hexane cracking activity. It was suggested that a Lewis acid–Brønsted acid interaction between the labile proton associated with the lattice aluminum and the extralattice aluminum species was responsible for the increase in the intensive factor. Beyerlein *et al.* (*8*) observed that the steaming of Y-zeolite treated with ammonium hexafluorosilicate, resulted in a catalyst with higher activity than USY materials with comparable lattice aluminum content. This was attributed to the lower amount of extralattice aluminum present in the conventionally prepared USY.

The presence of cations other than protons in the lattice can cause dramatic negative effects on the activity for H-Y zeolites (*9*). Beyerlein *et al.* (*10*) showed that residual sodium cations can poison zeolites to such an extent that isobutane cracking activity decreases drastically with only a small amount of sodium. Similarly, Hall and co-workers (*1*, *11*) reported ammonia poisoning studies on H-ZSM-5, H-Y zeolites, and H-mordenites, where they observed that converting a few percent of the Brønsted sites to NH_4^+ effectively completely poisoned the catalyst for paraffin cracking. Hall *et al.*(*1*d) and Fritz and Lunsford (*11*) reported similar observations using sodium poisoning. It was proposed by Fritz and Lunsford (*11*) that only a small fraction of sites were acidic enough to form carbenium ions, whereas, Hall and co-workers suggested that all the sites were being affected collectively by the introduction of additional electrons into the silica–alumina lattice.

These observations suggest that the intensive factor of acidity may not be as uniform as was envisaged in earlier reports and that dealumination can modify the zeolite lattice in ways which can in turn affect the acidity. The present work was undertaken to better define this phenomenon. H-Y zeolites having different amounts of extralattice aluminum, possibly in different forms, were prepared and thoroughly characterized using a variety of techniques. The objective was to identify the parameters that can affect the intensive factor of individual sites.

EXPERIMENTAL

Materials

A total of 15 Y-zeolites were used in this study. Five of these were commercial Y-zeolites obtained from Linde, viz., LZY-62, LZY-82, LZ210-6, LZ210-9, and LZ210-12. Commercial zeolites were exchanged with ammonium ions, except for LZY-82, which was already in the ammonium form. The remaining zeolites were prepared by dealumination of one of these commercial catalysts.

Prior to dealumination, the sodium content of the samples was first reduced by ion exchange with ammonium acetate. Approximately one gram of Y-zeolite was slurried with 3.5 *M* ammonium acetate solution and heated to reflux temperature with continuous stirring for 2 h. It was then washed with distilled, deionized water and dried at 100°C to a freely flowing powder. The NH_4-Y zeolite was subsequently converted into the hydrogen form by heating the catalyst to 400°C under flowing dry oxygen and then dry nitrogen for 3 h each.

Ammonium hexafluorosilicate (AHS) was used to dealuminate the catalyst up to a silicon to aluminum ratio (*R*) of 8. In a typical procedure, about 200 cc of 3.5 *M* ammonium acetate solution were added to 50 g of zeolite. The slurry was heated to 75°C and the stoichiometrically required amount of a 0.75 *M* AHS solution was added dropwise to the mixture. The addition rate was controlled to maintain a pH of 6. After 3 h the solution was cooled to room temperature, filtered, and washed repeatedly with an excess of distilled water.

Mild steam treatment was also used to dealuminate some of the zeolites. In a typi-

cal procedure, 10 g of zeolite were mixed with quartz chips and heated in flowing dry oxygen and dry nitrogen for 3 h at 400°C, respectively, under shallow bed conditions, i.e., where the height to diameter ratio of the zeolite bed was below 1.5. The temperature was raised to the desired dealumination temperature and nitrogen (1.25 cc/s) and steam (0.173 cc/s) were concurrently passed through the zeolite bed at atmospheric pressure. These conditions were maintained for 2 to 20 h (see Table 1).

Characterization

The pore volume of the zeolites was determined from the nitrogen uptake at 77°K and $p/p_0 = 0.05$. X-ray diffraction (XRD) patterns were obtained using a General Electric XRD5 diffractometer utilizing Cu$K\alpha$ radiation ($\lambda = 1.5418$ Å). The unit cell size (a_0) of the zeolites was estimated from the X-ray diffraction pattern using a methodology similar to ASTM procedure D 4932-85 (*12*) and using lead nitrate as an external standard. Samples were scanned from 2θ equal to 10° up to 60° and the X-ray diffraction line positions were determined within 0.005°. The variation in a_0 was related to the lattice Si/Al ratio using the correlation of Sohn *et al.* (*4*).

The total aluminum and sodium content of the zeolites were obtained by atomic absorption using a Perkin–Elmer 380 AA spectrometer. Approximately 100 to 250 mg aliquots of dry zeolite were calcined at 500°C, before dissolving in a mixture consisting of 10 cc HCl (37%), 2 cc H_2SO_4 (95%), and 25 cc HF (49%) and then heated to dryness. The remaining residue was completely dissolved in an additional 10 cc concentrated HCl, and diluted with 250 cc water for Al^{+3} determination or in 1000 cc H_2O for Na^+ determination. Two grams of potassium chloride were added to the solution to facilitate ionization. Commercial standard solutions of the respective element were used for calibration.

^{29}Si, ^{27}Al, and ^{1}H spectra were obtained by magic angle spinning (MAS) NMR using a Bruker MSL 300 spectrometer. ^{29}Si spectra were obtained from fully hydrated samples at 59.627 MHz, using a spinning rate of approximately 4 KHz, a 90° pulse length of 6 μs, and a repetition time of 10 s. Depending upon Si/Al ratio, from 200 to 10,000 scans were necessary to obtain a satisfactory signal-to-noise ratio. The ^{27}Al spectra were obtained at 78.205 MHz using a similar sample in a zirconia rotor. The spinning rate was maintained at 3 kHz to avoid the interference of spinning side bands with the main signal. The estimation of Al atoms by ^{27}Al NMR is subject to error due to quadrupolar line broadening. It is possible to minimize these effects, however, by applying very short pulses and small flip angles, to obtain mainly the central transitions (*13*). In this study a 10° flip by a 2-μs pulse was used. Typically 1000 scans were collected with a repetition time of 1 s. In order to favor a symmetric environment around the aluminum nucleus, all samples were fully hydrated under atmospheric conditions before acquiring the spectra (*13*). ^{27}Al chemical shifts were obtained with respect to aqueous aluminum nitrate as a reference, and aluminum phosphate was used as a quantitative standard to measure the amount of tetrahedral aluminum present in the lattice.

^{1}H spectra were obtained on fully dehydrated samples. The samples were pretreated overnight at 400°C, first in flowing dry oxygen and then in flowing dry nitrogen. The samples were then transferred into rotors in a glove bag under an inert atmosphere and the rotors sealed with a small amount of silicone grease. The rotors were stored under vacuum until needed. No change in the proton spectra was observed even after several days in storage. ^{1}H NMR spectra were acquired at 300 MHz and 4 kHz spinning speed, with a repetition time of 4 s. The empty rotor background was subtracted from the spectra acquired on the samples. Solid hexamethylbenzene was used for quantitative calibration. TMS solution was used as a chemical shift reference.

Reaction Studies

The cracking of *n*-pentane was studied using a fixed-bed reactor with a shallow catalyst bed having height-to-diameter ratio below 1.5. The typical catalyst loading was 65 mg and the F/W was 7.5×10^{-6} mol reactant $g^{-1}\,s^{-1}$. The catalyst particles, as stated by the manufacturer, had an average size below 1 μm. The zeolites were pretreated for 2 h each, at 400°C in flowing dry oxygen and then in flowing dry nitrogen. After pretreatment, nitrogen was bubbled through pentane in a saturator maintained at a constant temperature of 25 ± 0.5°C and flowed over the catalyst. The reaction was carried out at 400°C. On-line analysis of the product was carried out on a dual FID-TCD gas chromatography system, which allowed for the detection of hydrocarbons as well as hydrogen. Product concentrations were calibrated by using standard gas mixtures. Conversion rates were calculated as described by Englehardt and Hall (*11*b,c) from the carbon balance of the reaction products. This analysis was made using a column containing two packings in series (dibenzylamine and propylene carbonate on Chromosorb) thermostated at 0°C. An FID detector was used. Product concentrations were calibrated using standard gas mixtures. The data was treated as described in Ref. (*11*c).

TABLE 1

Summary of H-Y Zeolites Studied

Zeolites[a]	Lattice Si/Al	Pore volume (cc/g)	Preparation procedure
LZY-62	2.5	0.31	Commercial Y-zeolite, deaminated
LZY-82	5.1	0.30	Commercial ultrastable Y-zeolite, deaminated
LZ210-6	3.4	0.33	Commercial Y-zeolite, deaminated
LZ210-9	5.0	0.33	Commercial Y-zeolite, deaminated
LZ210-12	6.0	0.32	Commercial Y-zeolite, deaminated
D(Y62)3	2.9	0.32	AHS[b] treatment to LZ-Y62, 10 g, Y62, 50 cc, 3.5 *M* ammonium acetate, 12 cc, 0.4 *M* AHS
D(Y62)6	6.5	0.24	AHS treatment to LZ-Y62, 47.3 g, Y62, 190 cc, 3.5 *M* ammonium acetate, 133 cc, 0.7 *M* AHS
D(Y62)7	7.0	0.23	AHS treatment to LZ-Y62, 47.3 g, Y62, 190 cc, 3.5 *M* ammonium acetate, 133 cc, 0.75 *M* AHS
D(Y62)8	7.5	0.27	AHS treatment to LZ-Y62, 4.1 g, Y62, 16.4 cc, 3.5 *M* ammonium acetate, 5.7 cc, 1 *M* AHS
S(LZ12)7	7.3	0.32	Steaming of LZ210-12, 10 g, 100 Torr, 773 K, 100 min
S(LZ12)8	8.3	0.32	Steaming of LZ210-12, 10 g, 100 Torr, 773 K, 200 min
S(LZ12)10	9.7	0.32	Steaming of LZ210-12, 10 g, 100 Torr, 773 K, 300 min
S(LZ12)14	14.1	0.33	Steaming of LZ210-12, 10 g, 100 Torr, 773 K, 600 min, shallow bed treatment
S(LZ12)18	17.6	0.33	Steaming of LZ210-12, 10 g, 100 Torr, 773 K, 1200 min
S(D(Y62)6)18	18	0.31	AHS of LZY-62 followed by steaming of D(Y62)6, 10 g, 380 Torr, 873 K, 180 min

[a] For nomenclature, refer to text. The nominal Si/Al ratios are indicated by the final digits. When these data were supplied by the manufacturer, SiO_2/Al_2O_3 ratios are used.

[b] AHS: Ammonium Hexafluorosilicate.

RESULTS

Structural Characterization

The preparative procedures and framework Si/Al ratio for each Y-zeolite studied are summarized in Table 1. Three sets of catalysts were used. The first group was comprised of commercial zeolites obtained from Linde. These are designated as LZ-zeolites and their commercial names are retained. With LZ-210-6, 9, and 12, the last digits indicate the SiO_2/Al_2O_3 ratio. Elsewhere throughout this paper we have used Si/Al ratios which are approximately half the SiO_2/Al_2O_3 value. LZY-82 is a commercially available "ultrastable Y"; we are not certain about its evolution and therefore treat it separately with flags on the corresponding data points on the figures.

A second group was comprised of AHS-dealuminated catalysts and they are designated by letter D. A third group contained the steamed samples which are identified by the letter S. The symbols in the parenthesis represent the parent zeolite and the number after the parenthesis is the lattice Si/Al ra-

tio. For simplicity, when LZ210-12 was used as a parent sample it is indicated as LZ12.

The crystallinity and structure of all the zeolites involved in this work were monitored using XRD and pore volume measurements. All the characteristic XRD peaks corresponding to Y-zeolite structure were found to be present in all samples. The pore volumes measured at $P/P_0 = 0.05$ atm. are also listed in Table 1. Generally, the pore volume values were either in the vicinity of the theoretical value of 0.33 cc/g for Y-zeolites, or in a few cases significantly lower, close to 0.25 cc/g, suggesting that the pore system was partially filled by expelled alumina. This occurred with zeolites which were dealuminated to Si/Al ratio of 6 or above using AHS treatment. Steaming reopened the partially locked pore system of the AHS treated zeolites as evidenced by the restoration of full pore volume, e.g., in the S(D(Y62)6)18 sample.

Aluminum Content

The amount of lattice aluminum in the zeolites was determined independently using XRD lattice parameter measurements, ^{29}Si MAS-NMR, and ^{27}Al MAS-NMR. Figures 1A and 1B show the ^{29}Si and ^{27}Al NMR spectra, respectively, of LZY-62. These spectra were typical of all the zeolites. The batch of LZY-62 that we used for the present study clearly had some extralattice aluminum as evidenced by the octahedral signal near −4 ppm (Fig. 1B).

For the HY zeolites studied, at most six partially resolved signals were observed in the ^{29}Si NMR spectra, at chemical shifts between −89 and −110 ppm. The five signals have been assigned to framework silicon atoms with four to zero aluminum next-nearest neighbors, i.e., (OAl) groups (*14*, *15*). A weak sixth signal, upfield of the $Si(OAl)_0$ peak, was indicative of amorphous silica, and was sometimes observed in highly dealuminated zeolites (*14*). The relative intensities of these signals is thus a measure of the Si/Al ratio. The exact ratio was calculated from these spectra using the method developed by Engelhardt and coworkers (*14*). This could be converted into aluminum atom concentration, i.e., Al/g assuming unit cell compositions of $H_x(AlO_2)_x(SiO_2)_{192-x}$.

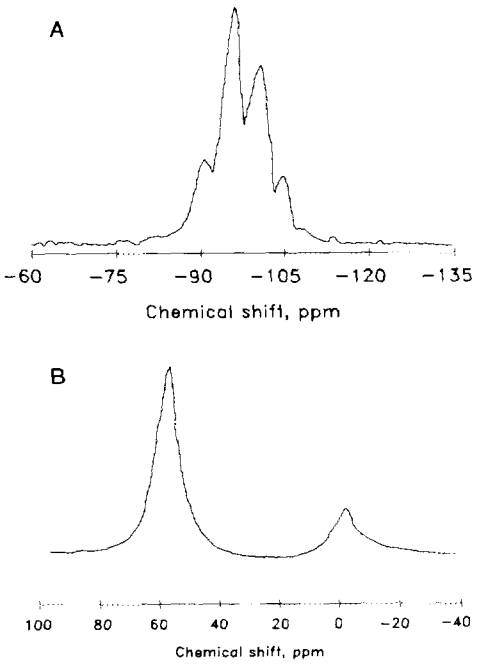

FIG. 1. (A) ^{29}Si and (B) ^{27}Al MAS-NMR spectra of the proton form of LZY-62 zeolite. Silicon atoms are surrounded by different number of aluminum atoms as follows: $Si(OAl)_4$ = −85 ppm, $Si(OAl)_3$ = −92 ppm, $Si(OAl)_2$ = −96 ppm, $Si(OAl)_1$ = −103 ppm, $Si(OAl)_0$ = −108 ppm, and amorphous Si = −111 ppm. Aluminum in tetrahedral, octahedral, and pentacoordination was observable near 56, −8, and 28 ppm, respectively. Samples were fully hydrated.

The ^{27}Al NMR spectra (Figure 1B) showed at most two signals, a signal at approximately 55 to 60 ppm corresponding to tetrahedrally coordinated aluminum and a signal at about 5 to -10 ppm corresponding to octahedrally coordinated aluminum. For determination of Si/Al ratio, it was assumed that all the tetrahedral signal originated from lattice aluminum. Thus quantitative integration of the tetrahedral signal was used to directly determine the Al concentration in the lattice.

TABLE 2

Aluminum Content of Y-Zeolites Determined by Various Techniques

Zeolite	Al atoms $\times 10^{-20}$/g						
	Lattice Al determined by				Total Al by AA	Extralattice Al[a]	Al_l-Na^{+}[b]
	XRD	^{29}Si NMR	^{27}Al NMR	Average			
LZY-62	28	29	26	28	31	3	25
LZY-82	19	16	14	16	26	10	16
LZ210-6	22	23	24	23	23	0	20
LZ210-9	16	17	18	17	18	1	15
LZ210-12	14	14	16	15	15	0	13
D(Y62)3	23	26	26	25	25	0	23
D(Y62)6	13	13	13	13	14	1	10
D(Y62)7	13	13	11	12	14	2	9
D(Y62)8	12	11	11	11	13	2	8
S(LZ12)7	11	12	12	12	14	2	11
S(LZ12)8	11	11	9	11	14	3	10
S(LZ12)10	9	9	9	9	13	4	9
S(LZ12)14	7	7	6	7	13	6	6
S(LZ12)18	4	5	6	5	12	7	4
S(D(Y62)6)18	6	5	5	5	6	1	4

[a] Values of extralattice Al are estimated to be accurate to $\pm 2 \times 10^{20}$ atoms/g; values for Na^{+} are estimated to be accurate to $\pm 1 \times 10^{20}$ ions/g.

[b] Al_l-Na^{+} was calculated by subtracting Na^{+} by AA from the average amount of lattice aluminum.

A comparison of the values of lattice aluminum obtained by the three different methods is made in Table 2. In general, there was a fairly good agreement among them. In order not to bias the discussion in favor of any one of the methods for determining lattice aluminum, an average of the three results was taken. This is also reported in Table 2. Extralattice Al was calculated by difference between the total and the average lattice Al. Also shown in Table 2 is the concentration of tetrahedral aluminum not neutralized by sodium ions, which can be considered to be that existing as Brønsted acid sites. It should be noted that for any parent zeolite the sodium content remained essentially constant throughout the treatments.

Table 2 also lists the *total* aluminum atom concentration as determined by atomic absorption (AA) analyses. In all cases the AA analysis gave aluminum contents that were equal to or larger than the average lattice aluminum concentration. Indeed in some cases, such as LZY-82 and S(LZ12)18, the total aluminum concentration as determined by AA was about twice as large as the lattice aluminum, indicating the presence of large amounts of extralattice or non-framework aluminum.

The numbers in Table 2 allow us to determine the concentration of extralattice aluminum by simply subtracting from the total aluminum determined by AA, the average value of lattice aluminum determined by the three independent methods. These values clearly demonstrate that although mild steaming effected dealumination, it did not effectively succeed in removing the extralattice aluminum from the crystallites. Indeed, a comparison of samples S(LZ12)7, S(LZ12)8, S(LZ12)10, S(LZ12)14, and S(LZ12)18, all of which were prepared from the same parent zeolite, show that although

increased steaming severity resulted in increased lattice dealumination, the alumina was not removed from the extralattice.

The concentration of octahedral aluminum in the zeolites was determined directly from the ^{27}Al spectra of fully hydrated samples (Table 3). In all cases the amount of octahedral aluminum was equal to or less than the amount of extralattice aluminum in the materials. It thus appears that several of the steamed zeolites contain nonoctahedral extralattice aluminum. In particular two zeolites, namely, LZY-82 and S(LZ12)18, contained large amounts of extralattice aluminum that could not be assigned to the octahedral form. While it is recognized that the quantitative determination of octahedral alumina can be plagued with the inaccuracies due to the quadrupolar moment of the ^{27}Al nucleus which can affect signal intensities (*13*), in the present work the spectral acquisition conditions were optimized to reduce these quadrupolar effects as detailed in the experimental section. Thus, these results strongly suggest that a significant portion of the extralattice aluminum cannot be accounted for and must exist in an asymmetric form unobservable by conventional ^{27}Al NMR measurements; we term this "NMR-invisible."

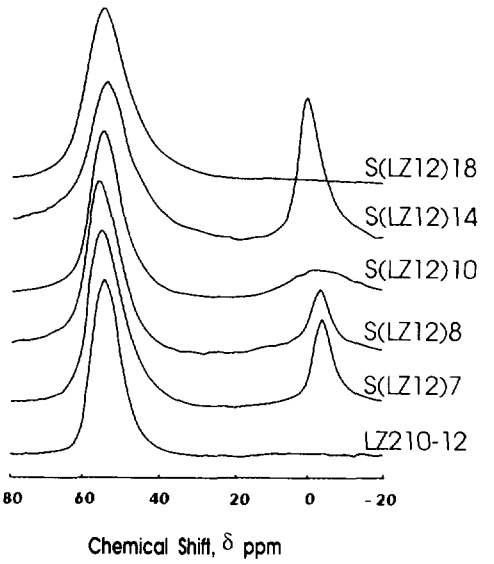

FIG. 2. Effect of the extent of steaming on the amount of octahedral aluminum formed as observed by ^{27}Al MAS-NMR on steamed H-Y zeolites. LZ210-12 was steam dealuminated under the conditions specified in Table 1.

TABLE 3

Extralattice Aluminum Content of H-Y Zeolites

Zeolite	Extralattice aluminum, Al atoms × 10^{-20}/g		
	Total[a]	Octahedral[b]	Other[c]
LZY-62	3	3	0
LZY-82	10	2	8
LZ210-6	0	0	0
LZ210-9	1	0	1
LZ210-12	0	0	0
D(Y62)3	0	0	0
D(Y62)6	1	0	1
D(Y62)7	2	1	1
D(Y62)8	2	0	2
S(LZ12)7	2	2	0
S(LZ12)8	3	2	1
S(LZ12)10	4	1	3
S(LZ12)14	6	6	0
S(LZ12)18	7	0	7
S(D(Y62)6)18	1	0	1

[a] By the difference between total aluminum obtained from AA and average lattice aluminum from XRD, ^{29}Si NMR, and ^{27}Al NMR.

[b] By quantitative ^{27}Al NMR.

[c] Other = Total − Octahedral.

Our results demonstrate that the exact dealumination procedure can strongly affect the amount and nature of the extralattice aluminum. Examination of Tables 2 and 3 clearly shows that significant amounts of extralattice aluminum were not formed in any of the zeolites dealuminated by using AHS treatment. In contrast, steaming invariably resulted in the formation of significant concentrations of extralattice aluminum. Interestingly it is this kind of treatment which leads to the formation of the highly acidic ultrastable preparations such as LZY-82.

Figure 2 shows the ^{27}Al MAS-NMR spec-

tra of LZ210-12 and the steam-dealuminated materials prepared from it. With increasing dealumination, the concentration of octahedral aluminum (excluding S(LZ12)14) initially increased and then decreased, whereas the total amount of extralattice aluminum, as given in Table 3, increased monotonically. Zeolite S(LZ12)18 shows little or no octahedral aluminum, although it can be argued that some octahedral aluminum may still be evident as a broad signal in the NMR spectrum. This pattern suggests that some of the octahedral aluminum is being converted to "NMR-invisible" aluminum as proposed by Klinowski *et al.* (*16*) with steaming treatment.

It should be noted that sample S(LZ12)14 was an exception to this pattern. Although dealumination did occur, extralattice aluminum remained in the form of octahedral aluminum. This sample, however, was dealuminated using a larger diameter column and hence a shallower catalyst bed. This demonstrates the sensitivity of the resulting structure to details of the preparation procedure.

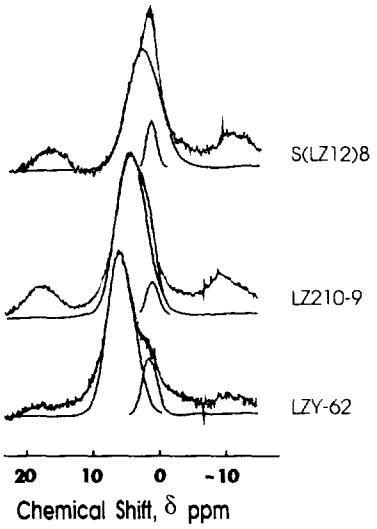

FIG. 3. ^{1}H MAS-NMR spectra of H-Y zeolites dehydrated at 400°C. The large signal is assigned to acidic protons and the small signal is assigned to terminal OH groups. Samples were dried at 400°C in oxygen and nitrogen for 4 h each. Spectra were collected on samples stored in sealed rotors.

Lattice Proton Concentration and Chemical Shifts

^{1}H-MAS-NMR spectra on typical H-Y zeolite samples are presented in Figure 3. In all the cases the spectra could be deconvoluted into two signals, the smaller one below 2 ppm and the larger at $2 < \delta < 7$ ppm. The smaller upfield signal at ca. 2 ppm contributed less than 10% of the total integrated signal. Pfeifer *et al.* (*17*) have reported three signals in ^{1}H MAS-NMR of H-Y zeolites. They assigned a signal at 1.8 ppm to OH silanol groups, and the other two signals to the acidic protons in different environments. Our results are generally consistent with their assignments. However, since our proton lines were much broader than those reported by Pfeifer, we were able to resolve only two signals in the dried samples. A third signal appeared when water was added.

A comparison is made in Figure 4 between proton concentration obtained from integration of the larger downfield signal only and sodium-free lattice aluminum in the H-Y zeolites. The fair agreement suggests that each acidic proton is associated with a lattice aluminum. Extralattice aluminum may affect acid strength, but does not significantly contribute to the number of Brønsted sites. In the case of steam dealuminated zeolites, some disagreement between proton content and sodium free lattice aluminum content was observed.

Reaction Studies

The overall activity of the catalysts towards cracking of *n*-pentane was used as a measure of total acidity. This is justified in separate papers where a detailed description of these results are to be published (*18*). The initial reaction rate characteristically was high, but it decreased rapidly with time reaching a pseudo-steady-state after about 3 h. The total conversion in this lined-out state was used for the comparison of the

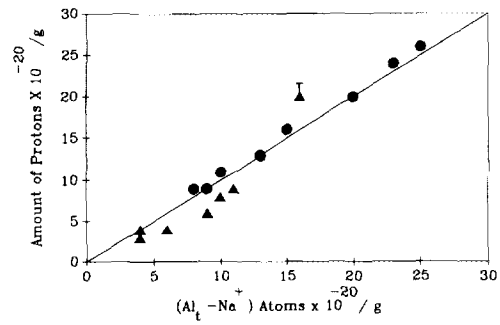

FIG. 4. Relationship between proton and lattice (Al_t-Na^+) content in H-Y zeolites. Lattice aluminum content listed in Table 2, was obtained as an average from XRD, ^{29}Si, and ^{27}Al NMR. Proton content was obtained from ^1H MAS-NMR. ●, commercial and AHS treated; ▲, Steamed, and Ⱥ, LZY-82.

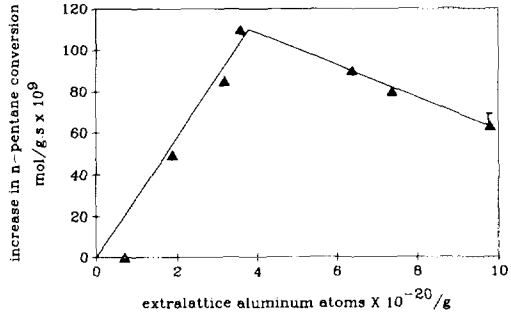

FIG. 6. Effect of the amount of extralattice aluminum on increase in *n*-pentane cracking activity in steamed H-Y zeolites.

catalysts. In all cases hydrogen was observed only in the initial stages of the reaction when the activity was high. In addition to cracking, isomerization to isopentane was the major reaction.

Figure 5 is a plot of the reaction rate for the various catalysts as a function of concentration of sodium free lattice aluminum atoms, i.e., lattice Brønsted acid sites. Two groupings of catalysts can be discerned in this figure. One of the groups consisted of LZY-62, the LZ-210 series, and catalysts prepared from LZY-62 by AHS treatment.

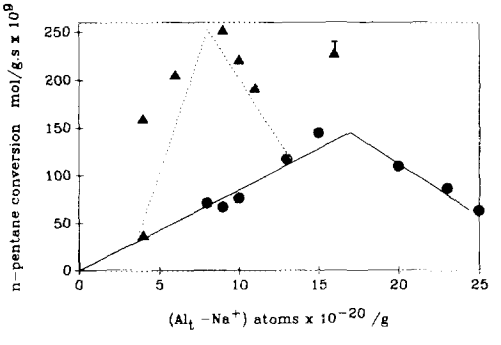

FIG. 5. Effect of cation-free lattice aluminum on the *n*-pentane cracking activity in H-Y zeolites. Reaction temperature was 400°C, catalyst loading was 0.065 g, and *F*/*W* was 7.5×10^{-6} mol/g/s. ●, commercial and AHS treated; ▲; steamed; Ⱥ, LZY-82.

For these catalysts, the *n*-pentane cracking activity followed a pyramidal relationship where activity increased linearly with lattice aluminum concentration up to (Al_t-Na^+) = 17×10^{20} atoms/g (32 Al_t/unit cell) and then decreased. This behavior has been reported for a limited series of HY zeolites by Lunsford and co-workers (*4*). The second group consisted of LZY-82 and catalysts prepared from LZ210-12 by steam dealumination. For these catalysts the activity in all cases was considerably higher than for the first group, and a maximum activity was observed at a lattice aluminum content of 8×10^{20} (Al_t-Na^+) atoms/g zeolite. This group of Y-zeolites was found to contain appreciable quantities of extralattice aluminum. These results are in agreement with similar observations made for a series of HZSM-5 catalysts by Haag and co-workers (*5*). The effects of extralattice aluminum on the activities of steamed samples is shown in Fig. 6. Catalyst LZY-82 had a similar elevated activity which could be further enhanced by mild steaming (*8a*, *10*).

DISCUSSION

Clear differences appeared in both structure and catalytic activity of the various zeolites as a result of the dealumination procedure. These differences may be better understood in terms of the dealumination mechanisms that have been proposed. Breck and co-workers (*19*) have suggested

that during AHS dealumination silicon atoms may migrate into the vacancies created by the removal of aluminum ion–cation pairs. Thus, AHS treatment was characterized as a replacement of the aluminum by silicon, thereby producing zeolites with intact crystallinity. In this process the aluminum removed is water soluble and may be washed out, resulting in minimal extralattice aluminum. Indeed, very little octahedral aluminum was observed in the ^{27}Al NMR spectra for the LZY-210 series or D(Y62)3, suggesting that this dealumination technique can lead to ideal Y-zeolites with almost perfect lattice structure. Thus, *mild* AHS dealumination produced Y-zeolites with an ideal pore structure and negligible amounts of extralattice aluminum. More severe dealumination beyond Si/Al = 6 however, resulted in the formation of extralattice aluminum, as evidenced by the appearance of octahedrally coordinated aluminum and reduced pore volumes. This was consistent with the reports of Garralon *et al.* (*20*). Thus, in these cases agglomerates of extralattice aluminum evidently occurred resulting in pore blocking and the observed reduction in pore volume. In some cases the observed decrease in pore volume is so high compared to the amount of extralattice aluminum present that other amorphous material, such as some of the silica observed by ^{29}Si NMR, may also have been partly responsible.

All the commercial zeolites and steamed zeolites were found to have pore volumes close to the value calculated from the crystal structure (0.33 cc/g). This is surprising in view of the significant amount of extralattice aluminum detected in LZY-82 and in other steamed Y zeolites. Evidently, the extralattice aluminum is not present in the pore system as with the AHS-treated zeolites, but either in a finely dispersed form or is outside the pore structure so as not to affect the pore volume. Further evidence for this speculation has been obtained using ^{129}Xe NMR where no decrease in the mean-free-path of the Xe was noted with steaming (*18*). It should also be noted that the zeolites containing this form of extralattice aluminum exhibited enhanced activity for *n*-pentane cracking (Fig. 5). Therefore, it may be that this alumina is reconstituted into the structure inside the β-cages in a way which "promotes" the remaining Brønsted sites.

Steaming of the low-pore-volume material D(Y62)8 to S(D(Y62)8)18 apparently reopened the pore system, showing that it was simply partially blocked, rather than structurally collapsed during AHS treatment. Evidently, any amorphous material formed during an AHS treatment was removed during steaming, thereby restoring the original pore volume. In this case the removal of extralattice material was almost complete and the catalytic activity did not increase on steaming (Figs. 5 and 6). These results suggest that extralattice aluminum can be removed by steaming, although the exact mechanism of this removal is not clear.

Clearly the dealumination treatment affected both the amount and nature of extralattice aluminum in the zeolites. Using *n*-pentane cracking as a measure of acidity it can be seen that the steamed-dealuminated materials (which exhibited higher cracking activity than the AHS-treated samples) may be presumed to have higher acidity. Interestingly this has occurred while lowering the total alumina and lattice alumina contents, i.e., the intensive factor of the acidity has been increased, not the extensive factor. Since significant amounts of extralattice aluminum were detected in the steamed materials, this suggests a role of the extralattice aluminum in acidity.

The lattice Si/Al ratio determined by the various techniques were in good agreement with each other. In particular the XRD correlation was found to be valid irrespective of the extralattice aluminum content, although some minor deviation was observed for LZY-82 which contained a large amount. Since the XRD correlation stems from the measurement of lattice parameters, the extralattice aluminum evidently does not inter-

fere with the lattice geometry to an appreciable extent. Thus, any effect of the extralattice aluminum on the acid properties must relate to chemical interactions and cannot be due simply to geometric changes in the lattice.

The proton contents obtained from quantitative proton NMR were in good agreement with the number of sodium-free lattice aluminum atoms as shown in Fig. 4. This suggests that almost all the protons are associated with lattice aluminum and only a negligible amount of hydrogen may have been incorporated into extralattice aluminum species. The latter may be viewed as Lewis-type material (*21*).

The points for the proton content of the steam dealuminated zeolites (▲), as measured by ^{1}H NMR, generally fell below the line for all the data. One possible explanation is that some of the lattice charge associated with the lattice alumina is being compensated by a positively charged species other than protons, perhaps a species formed from the extralattice aluminum.

Several forms of extralattice alumina have been proposed in the literature, such as boehmite (*22, 23*), pseudo-boehmite, and AlO^+ species (*21*). In the present work, the amount of extralattice alumina in steamed samples was occasionally found to be as high as 60% of the total aluminum content. Additionally, the difference between total aluminum and lattice aluminum content was sometimes higher than the octahedral aluminum content observed by ^{27}Al NMR. Thus, octahedral aluminum cannot account for all the extralattice alumina and an "NMR-invisible" extralattice form must also be present. This "NMR-invisible" aluminum could in some cases account for as much as 75% of the total extralattice alumina.

The nature of the "NMR-invisible" aluminum is not clear. It has been demonstrated that a five-coordinated aluminum (*24*) or a distorted tetrahedral aluminum (*25*) gives a distinct signal between those corresponding to a four- and a six-coordinated aluminum. Such a signal was not observed in any of the zeolites under investigation. Because of the quadrupole moment of the aluminum nucleus, it is possible that other alumina coordinations, if present, have a low enough symmetry so as to be unobservable by NMR. The salient point is, however, that this form of alumina can enhance the catalytic activity.

It has been argued that all the acid sites in silica-rich zeolites have the same intensive factor of acidity (*2, 4, 5, 8*), i.e., all acid sites have equal acid strength. This is easy to conceptualize as the sites are fairly far apart and cannot readily interact with each other. In these cases the total acidity should increase linearly with lattice aluminum content. As the aluminum content increases further, a point is reached where the second nearest neighbor interactions become common, i.e., the aluminum atoms come close enough to each other to interact electronically, causing electron density to shift towards the O–H bond associated with the aluminum atoms. This would lead to a reduction in the intensive factor of acidity and hence, in a decrease in total activity. Indeed, using *n*-pentane cracking as a measure of acidity this behavior was observed for zeolites with little or no extralattice alumina, as shown in Fig. 5. A maximum in catalytic activity for these structurally pure zeolites was observed at $(Al_l\text{-}Na^+) = 17 \times 10^{20}$ atoms/g, in accordance with the model suggested by Dempsey (*26*) and later by Barthomeuf (*29*) and Mikovsky and Marshall (*27*). Clearly, poisoning by Na^+ (*9–11*) or conversion of Brønsted acid protons into NH_4^+ (*1*) ions produce similar long range electronic effects.

Some of the zeolites dealuminated by ammonium hexafluorosilicate, such as D(Y62)8, were found to contain a small but detectable quantity of extralattice alumina. Their activity, however, was not affected. As previously discussed, it is likely that this extralattice alumina is present in the form of large agglomerates. The lack of effect of these agglomerates on activity suggests that

they may be in the form of neutral AlO_x species which do not interact with the Brønsted acid centers.

Not all zeolites exhibited the same activity pattern. A group of mildly steamed zeolites, mainly S(LZ12)7, S(LZ12)8, S(LZ12)10, S(LZ12)14, and S(LZ12)18 and the commercial ultrastable LZY-82 zeolite, showed higher activity relative to other zeolites. Their activity pattern can be represented by a second inverted V-shaped curve with a maximum in catalytic activity for $(Al_t - Na^+) = 8 \times 10^{20}$ atoms/g. This behavior is reminiscent of that described for mildly steamed HZSM-5 (*5*).

LZY-82 is a commercially available ultrastable Y-zeolite. The rest were steam dealuminated under mild conditions. As has been discussed, such steaming results in the formation of highly dispersed extralattice alumina in a reconstituted structure as shown by the constant pore volume values regardless of the amount of extralattice alumina.

Figure 6 shows the relationship between the amount of extralattice alumina and the absolute increase in the *n*-pentane cracking activity relative to the line defined by AHS-treated samples. A "volcano-type" behavior is observed with a maximum corresponding to an extralattice alumina content of 4×10^{20} Al atoms/g. This type of behavior supports the idea of extralattice alumina enhancing the acidity of existing Brønsted acid sites, since the enhanced activity pattern appears to be independent of the lattice aluminum content. Interestingly the effect of "crowding" of these sites is also apparent as the enhancement passes through a maximum.

No direct correlation was observed between the increase in activity and the various individual forms of extralattice alumina, such as octahedrally coordinated or "NMR-invisible" extralattice alumina found in the steamed samples. It appears that the extralattice alumina in all various forms are able to collectively contribute to an increase in the catalytic activity.

CONCLUSIONS

This work has shown that extralattice alumina in H-Y zeolites can be produced in different forms depending on the preparation history of the catalyst. AHS dealumination can produce a clean Y-zeolite by reducing the formation of extralattice alumina. It was also observed that mild dealumination conditions can produce extralattice alumina, predominantly in octahedral form. With an increase in the severity of steam dealumination conditions extralattice alumina is converted into an "NMR-invisible" form which is not in tetrahedral, octahedral, or pentacoordination. A low coordination or a severely distorted tetrahedral coordination are suggested as possibilities. Conceivably this is located inside the β-cages located on six rings and bridge-bonded via oxygen to another such ion on an adjustant ring.

It has been previously demonstrated that Brønsted acidity is essentially associated with lattice aluminum and is predominantly responsible for the catalytic activity in H-Y zeolites. The extralattice alumina seems to be in a form that does not contribute to the Brønsted acidity. Hence does not directly affect the activity, but it certainly does enhance the acidity and raises the catalytic activity. The type of interaction with the lattice aluminum may be as suggested by Lago *et al.* (*5*). Both ^{27}Al NMR visible and invisible extralattice alumina were found to contribute to the enhancement in acidity in steam dealuminated zeolites.

It was determined that the maximum catalytic cracking activity can be assigned to a definite value of lattice aluminum only for structurally pure zeolites, and the presence of extralattice aluminum altered the position of the activity maximum (see Fig. 5). On mildly steaming, the position of this maximum will likely depend on the Si/Al ratio of the parent material. Thus, an optimum combination of lattice aluminum atoms, which represent Brønsted acid sites, and extralattice aluminum species was observed to correspond to the maxi-

mum catalytic activity. These observations suggest that all Brønsted acid sites may have more or less the same acid strengths, but that association with extralattice aluminum may be collectively affecting the intensive factor of the Brønsted acid centers. Crowding of Brønsted acid sites or extralattice aluminum resulted in a decrease in catalytic activity.

Finally, it should be noted that this work presents a description of controlled dealumination to prepare materials with systematically increasing Si/Al ratios and controlled amounts of extraframework aluminum.

ACKNOWLEDGMENT

Support of this work by the Department of Energy under Grant DE-FG02-87ER13774 is gratefully acknowledged.

REFERENCES

1. (a) Lombardo, E. A., Sill, G. A., and Hall, W. K., *J. Catal.* **119,** 426 (1989); (b) Lombardo, E. A., Hall, W. K., *J. Catal.* **112,** 565 (1988); (c) Hall, W. K., Lombardo, E. A., and Engelhardt, J., *J. Catal.* **115,** 611 (1989).
2. (a) Aronson, M. T., Gorte, R. J., and Farneth, W. E., *J. Catal.* **98,** 434 (1986); (b) Gorte, R. J., and Aronson, M. T., in "Proceedings of 10th North American Meeting of the Catalysis Society," 1986.
3. Uytterhoven, J. B., Christ, L. G., and Hall, W. K., *J. Phys. Chem.* **69,** 2117 (1965).
4. (a) Sohn, J. R., DeCanio, S. J., Fritz, P. O., and Lunsford, J. H., *J. Phys. Chem.* **90,** 4847 (1986); (b) DeCanio, S. J., Sohn, J. R., Fritz, P.O., and Lunsford, J. H., *J. Catal.* **101,** 132 (1986); (c) Sohn, J. R., DeCanio, S. J., Lunsford, J. H., and O'Donnell, D. J., *Zeolites* **6,** 225 (1986); (d) Lunsford, J. H., *ACS Meet. Div. Pet. Chem.* **31**(4), 654 (1990); (e) Fritz, P. O. and Lunsford, J. H., *J. Catal.* **118,** 85 (1989).
5. (a) Lago, R. M., Haag, W. O., Mikowski, R. J., Olson, D. H., Bellring, S. D., Schmitt, K. D., and Kerr, G. T., *New Dev. Zeolite Sci. Technol.* **28,** 677 (1986); (b) Haag, W. O., and Dessau, R. M., *in* "Proceedings, 8th International Congress on Catalysis, Berlin, 1984," Vol. 2, p. 304. Dechema, Frankfurt am Main, 1984; (c) Haag, W. O., Lago, R. M., and Weiss, P. B., *Nature* **309,** 589 (1984); (d) Haag, W. O., *in* "Proceedings, 6th International Zeolite Symposium, Tokyo," p. 466. Butterworths, London, 1984.
6. Lunsford, J. H., *J. Phys. Chem.* **72,** 4163 (1968).
7. Miradatos, C., and Barthomeuf, D., *J. Chem. Soc. Chem. Commun.*, 39 (1981).
8. (a) Beyerlein, R. A., McVicker, G. B., Yacullo, L. N., and Ziemiak, J. J., *J. Phys. Chem.* **92,** 1967 (1988); (b) McVicker, G. B., Kramer, G. M., and Ziemiak, J. J., *J. Catal.* **83,** 286 (1983).
9. (a) Dyer, A., and Singh, A. P., Zeolites **8,** 242 (1988); (b) Dyer, A., *in* "Motivations in Zeolite Materials Science" (P. J. Grobet *et al.*, Eds.) p. 333 ff. Elsevier, Amsterdam, 1988.
10. Beyerlein, R. A., McVicker, G. B., Yacullo, L. N., and Ziemiak, J. J., *ACS Meet. Div. Pet. Chem.* **31,** 190 (1986).
11. (a) Fritz, P. O., and Lunsford, J. H., *J. Catal.* **115,** 85 (1989); (b) Hall, W. K., Engelhardt, J., and Sill, G. A., *in* "Proceedings, 8th International Zeolite Conference, Amsterdam," pp. 1253–1262, 1990; (c) Hall, W. K., and Engelhardt, J., *J. Catal.* **125,** p. 472 (1990).
12. "Annual Book of ASTM Standards," Vol. 05.03, p. 675, D3942-85 (1987).
13. Hamadan, H., Sulicowski, B., and Klinowski, J., *J. Phys. Chem.* **93,** 350 (1989).
14. (a) Engelhardt, G., Lohse, U., Magi, M., and Lippmaa, E., *in* "Structure and Reactivity of Modified Zeolites" (P. A. Jacobs *et al.*, Eds.), p. 23. Elsevier, Amsterdam, 1984; (b) Engelhardt, G., Lohse, U., Magi, M., Tarnak, M., and Lippmaa, E., *Z. Anorg. Allg. Chem.* **482,** 49 (1981).
15. Klinowski, J., Ramdas, S., Thomas, J. M., Fyfe, C. A., and Hartman, J. S., *J. Chem. Soc. Faraday Trans. 2,* **78,** 1025 (1982).
16. Klinowski, J., Fyfe, C. A., and Gobbi, G. C., *J. Chem. Soc., Faraday Trans.* **1,** 81, 3003 (1985).
17. (a) Pfeifer, H., Freud, D., and Hunger, M., *Zeolites* **5,** 274 (1985); (b) *Chem. Phys. Lett.* **105,** 427 (1984); (c) *Z. Phys. Chem. NF,* **152,** 171 (1987).
18. (a) Shertukde, P. V., Marcelin, G., Sill, G. A., and Hall, W. K., *J. Catal.* **136,** 446 (1992); (b) Shertukde, P. V., Hall, W. K., and Marcelin, G., *Catal. Today,* **15,** 491 (1992).
19. (a) Breck, D. W., Blass, H., and Sleeks, G. W., US. Patent No. 4 503 023, (1985); (b) Jacobs, P. A., and Uytterhoeven, J. B., *J. Catal.* **22,** 193 (1971); (c) Scherzer, J., Bass, J. L., *J. Catal.* **28,** 101 (1973); (d) Scherzer, J., "Structure and Reactivity, ACS Monograph No. 248, p. 157, Washington, DC.
20. Garralon, G., Fornes, V., and Corma, A., *Zeolites* **8,** 268 (1988).
21. (a) Kuhl, G. H., *ACS Symp. Ser.* **40,** 96 (1977); (b) Kuhl, G. H., "Molecular Sieves" (J. B. Uytterhoeven, Ed.), p. 227, Lueven University Press, 1973.
22. Loewenstein, W., *Am. Mineral.* **39,** 92 (1954).
23. Shannon, R. D., Gardner, K. H., Staley, R. H., Bergeret, G., Gallezot, P., and Auroux, A., *J. Phys. Chem.* **89,** 4778 (1985).
24. (a) Alemany, L. B., and Kirker, G. W., *J. Am. Chem. Soc.* **108,** 6158 (1986); (b) Gilson, J. P., Ed-

wards, G. C., Peters, A. W., Rajgopalan, K., Wormsbecher, R. F., Roberie, T. G., and Shatlock, M. P., *J. Chem. Soc. Chem. Commun.*, 91 (1987).

25. Samoson, A., Lippmaa, E., Engelhardt, G., Lohse, U., and Jerschkewitz, H. G., *Chem. Phys. Lett.* **134,** 589 (1987).
26. (a) Dempsey, E., *J. Catal.* **39,** 155 (1975); (b) *J. Catal.* **33,** 497 (1974).
27. Mikovsky, R. J., and Marshall, J. F., *J. Catal.* **44,** 170 (1976).
28. Jacobs, P. A., *Catal. Rev. Sci. Eng.* **24**(3), 415 (1982).
29. Barthomeuf, D., *Mater. Chem. Phys.* **17,** 49 (1987).